Journal of Alloys and Compounds 489 (2010) 339–342

Contents lists available at ScienceDirect

Journal of Alloys and Compounds

journal homepage: www.elsevier.com/locate/jallcom

Sn-flux syntheses, characterizations and bonding analyses of OsB and TiB_2

Boniface P.T. Fokwa*, Patrick R.N. Misse, Michael Gilleßen, Richard Dronskowski

Institute of Inorganic Chemistry, RWTH Aachen University, D-52056 Aachen, Germany

ARTICLE INFO

Article history:
Received 24 June 2009
Received in revised form
14 September 2009
Accepted 22 September 2009
Available online 30 September 2009

Keywords:
Binary borides
Tin flux synthesis
Crystal structure
COHP bonding

ABSTRACT

Single-phase crystalline powder of the technologically important TiB_2 and powder of OsB have been successfully synthesized at moderate temperature (900 °C) using metallic tin as a melting agent. The structural relationship between both phases is discussed. COHP bonding analyses show strong B–B interactions in TiB_2 but no such in OsB. The bonding situation in both phases is also compared with that of $Ti_{1.6}Os_{2.4}B_2$ and $Ti_{1.6}Os_{1.4}RuB_2$ phases. TiB_2 and OsB are metallic conductors according to DOS curves.

1. Introduction

In recent years binary metal borides have gained an increasing interest both theoretically and experimentally, owing to their remarkable physical, chemical and mechanical properties. In particular, superhard materials are of great industrial importance with applications such as abrasives, coatings and cutting tools [1].

Lately, borides of osmium have been the focus mainly within the theoretical community, because it has been found that metallic osmium has a bulk modulus close to that of diamond [2–6], but with a much lower hardness because of its pure (and weak) metallic bonds. Therefore increasing the bond strength of osmium by adding light elements (boron, carbon) may increase the hardness of the so-obtained material compared to that of pure osmium. However, only three phases ($OsB_{1.1}$, Os_2B_3 and OsB_2) were discovered in the Os–B system by the time [7]. A few years ago, OsB was predicted to be stable in the WC-type structure [8,9], confirming an earlier theoretical prediction [10]. More importantly its mechanical properties were also predicted [8,9]. In the last year (2008) the synthesis of OsB was achieved by arc-melting the elements, and the predicted structural and mechanical properties (hard and ultra-incompressible) were confirmed [11].

On the other hand, more phases (Ti_2B, TiB, Ti_3B_4, TiB_2, $Ti_{0.84}B_{25}$ and $Ti_2B_{103.3}$) have been discovered in the Ti–B system [7]. Polycrystalline ceramics based on TiB_2 have received considerable attention as electrodes for liquid aluminum, cutting tools, and wall materials for nuclear fusion [12]. Although TiB_2 has now been known for more than six decades, its synthesis is still unsatisfactory, and several synthetic routes have been proposed [12,13]. The synthesis of TiB_2 powder is mostly based on high-temperature methods, for example, the carbothermal reduction of titanium oxide (rutile) and boric acid with temperatures above 1800 °C [12]. This reaction is, however, highly endothermic and therefore makes the commercial TiB_2 synthesis very expensive as a consequence of the very high operating temperature. Consequently, a lower-temperature route for preparing TiB_2 is imperatively needed. In the last year (2008) two different methods for the preparation of TiB_2 powders were reported, but both were performed at temperatures up to 1400 °C [14,15].

Syntheses in metal fluxes have a huge potential for generating new intermetallic species at moderate temperatures, and recently many new phases, sometimes with very unusual compositions, have been prepared by this method [16]. Although TiB_2 was already synthesized by this method using different metal flux agents (aluminum [17], iron, nickel, cobalt [18] and copper [19]), its synthesis was carried out at temperatures of at least 1200 °C. The present report describes the results of the syntheses at a moderate temperature as regards to both the technologically important titanium diboride and the recently discovered ultra-incompressible osmium boride using metallic tin as a flux-melting agent. In addition, the crystal structures of both phases are compared, and their bonding situation is quantified using COHP bonding analyses.

2. Experimental

2.1. Synthesis and EDX analysis

OsB and TiB_2 were synthesized in a tin flux. The elemental powders of osmium (powder, 99.9%, Degussa) or titanium (powder, 99.9%, Degussa) and crystalline

* Corresponding author. Fax: +49 2418092642.
E-mail address: boniface.fokwa@ac.rwth-aachen.de (B.P.T. Fokwa).

0925-8388/$ – see front matter © 2009 Elsevier B.V. All rights reserved.
doi:10.1016/j.jallcom.2009.09.125

Table 1
Rietveld refinement results of the X-ray powder pattern of OsB product obtained from Sn-flux synthesis.

Formula; molecular weight	OsB; 201 g/mol
Measurement range; increment	$6^\circ \leq 2\theta \leq 100^\circ$; 0.005°
Temperature	298 K
Structure refinement	RIETVELD, least squares method
Profile function	Pseudo-VOIGT
Lattice parameters	$a = 2.8767\ (2)$ Å
	$c = 2.8718\ (2)$ Å
Space group	P–6m2
R_{Bragg}	0.048
R_F	0.090
Phase yield	≈ 80% (Os: ≈ 20%)

boron (pieces, 99.999%, Alfa Aesar) were weighed in the respective ratios according to their formulas. After weighing, the powders were mixed by a dry process using a mortar and a pestle. Pure powder of tin (99.99%, Merck) was used as a flux-melting agent and added in a TiB_2:2Sn or OsB:2Sn weight ratio. The mixed powders were put into an alumina tube and placed in a quartz glass ampule. After evacuation the ampule was filled with argon and positioned in a programmable stainless-steel tube-furnace for reaction. The heating conditions in the Ar atmosphere were as follows.

First, the mixture was heated slightly above the melting point of tin (300 °C) with a heating rate of 10 °C min^{-1}. After holding this temperature for 12 h, the sample was slowly heated to 900 °C with a heating rate of 2 °C min^{-1}, held for 48 h and then slowly cooled to room temperature with a cooling rate of 2 °C min^{-1}. The obtained powders were leached out into a small beaker using concentrated hydrochloric acid (37%) at room temperature to remove the flux-melting agent (Sn). Finally, deionized water and acetone, respectively, were added to wash the remaining solid. Dark-gray and black fine powders were obtained as final products for OsB and TiB_2, respectively.

The chemical compositions were checked by energy dispersive X-ray analysis (EDX) on a high-resolution, low-energy SEM of the type LEO 1530 (Oberkochen, Germany) equipped with an EDX system of the type INCA (Oxford, England). No other metal than those used was found from these EDX analyses. In the case of TiB_2 no detectable amount of tin could be recorded in the product which had been preliminarily treated with concentrated hydrochloric acid.

2.2. Structural characterization

X-ray powder diffraction (XRD) patterns were recorded on a Huber-Guinier 670 X-ray diffractometer with Cu Kα_1 radiation ($\lambda = 1.54059$ Å) and a Ge monochromator. The lattice parameters and the atomic positions were refined (see Table 1) on the basis of powder data using the program Fullprof [20].

2.3. Theoretical methodology

Electronic-structure calculations were carried out based on the all-electron scalar-relativistic Linear Muffin-Tin Orbital (LMTO) theory [21,22] in its tight-binding representation [23] using the TB-LMTO-ASA 4.7 program [24]. For the density-functional parametrization of exchange and correlation, the scheme by Vosko, Wilk, and Nusair [25] was utilized and augmented with gradient corrections [26] such as to follow the generalized-gradient approximation (GGA). A $24 \times 24 \times 16$ k-mesh for OsB and a $19 \times 19 \times 25$ k-mesh for TiB_2 was used. The chemical bonding was investigated using the Crystal Orbital Hamilton Population (COHP) analysis [27], which is an energy-resolved partitioning technique of the band structure energy (sum of the Kohn–Sham eigenvalues) in terms of atomic and bonding contributions [28].

3. Results and discussion

Figs. 1 and 2 show the Rietveld refinement curve for OsB and comparative X-ray powder patterns of the TiB_2 product, respectively. TiB_2 was single phase (Fig. 2), whereas the OsB product contains unreacted elemental osmium (about 20%). The lattice parameters obtained, $a = 2.8767(2)$ Å and $c = 2.8718(2)$ Å for OsB and $a = 3.0295(5)$ Å and $c = 3.2291(4)$ Å for TiB_2, are in very good agreement with the reported values.

OsB was synthesized for the first time using a metal flux method (Sn flux), in contrast to TiB_2 which was already successfully synthesized by this method (other authors) but using different metal flux agents (aluminum [17], iron, nickel, cobalt [18] and copper [19]). However, the main advantage of the Sn-flux synthesis is the

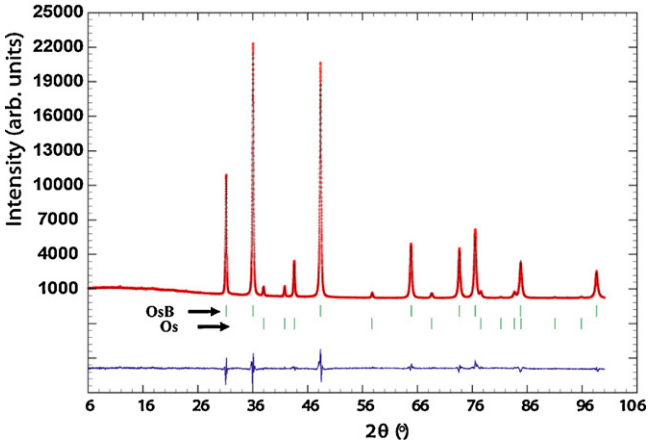

Fig. 1. Rietveld refinement of the X-ray powder pattern of the OsB-product showing measured and fitted intensities (top), the position of the Bragg peaks for OsB and Os (middle), and the difference intensity curve (bottom).

temperature of synthesis (900 °C) which is the lowest for a TiB_2 synthesis until now. In fact using the above mentioned flux agents the temperature of synthesis was 1200 °C (Cu flux), 1450 °C (Al flux) and 1600–1750 °C (Fe, Co, Ni fluxes).

OsB crystallizes with the WC-type structure (space group P–6m2). The structure is built up of face-sharing trigonal prisms of osmium atoms (see Fig. 3a), but only one out of two trigonal prisms can be occupied by boron because the distance between both prism centers is too short (≈1.6 Å) for a B–B bond (e.g. 1.8–1.9 Å in orthorhombic OsB_2 [29]). Therefore only two types of bonding interactions should be present in the structure: Os–B and Os–Os.

According to the COHP curves (see Fig. 4a, left) the Os–B interactions are optimized in OsB: bonding orbitals are filled and antibonding orbitals are empty. The Os–Os pair, however, shows antibonding orbitals near and at the Fermi level. Therefore this COHP bonding analysis suggests that it is the Os–B interaction that creates the structural stability of OsB, as expected. In agreement with this assessment the energy integral ICOHP for an

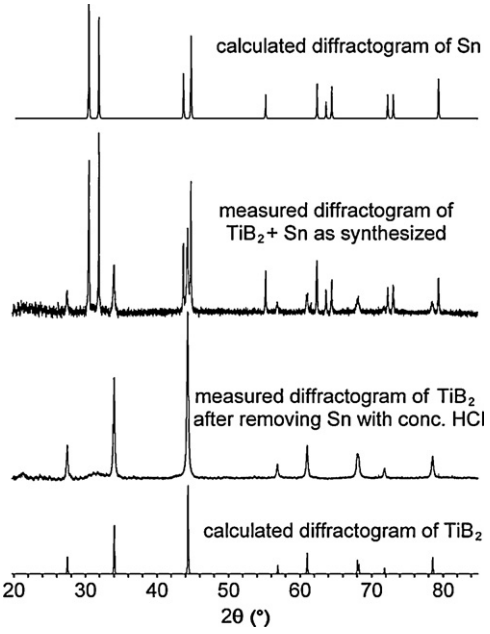

Fig. 2. Comparisons of calculated and measured X-ray powder patterns from the TiB_2 synthesis (using a Sn-Flux). Single-phase TiB_2 was obtained (second pattern from bottom).

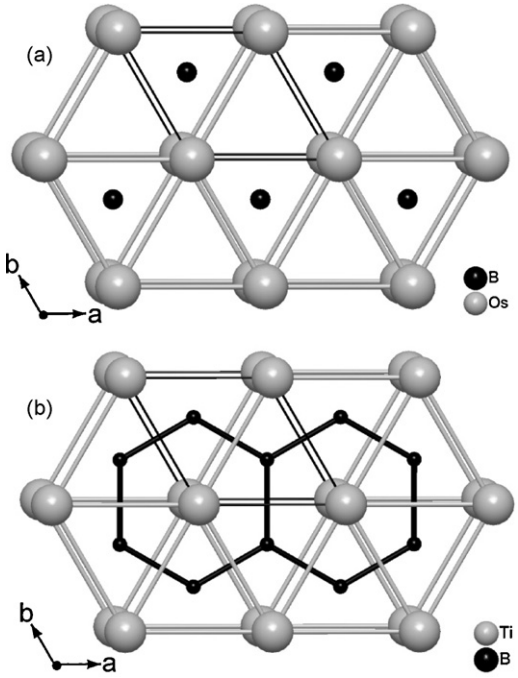

Fig. 3. Projection of the crystal structures of OsB (a) and TiB_2 (b) nearly along [0 0 1]. The solid black parallelepipeds represent the unit cells.

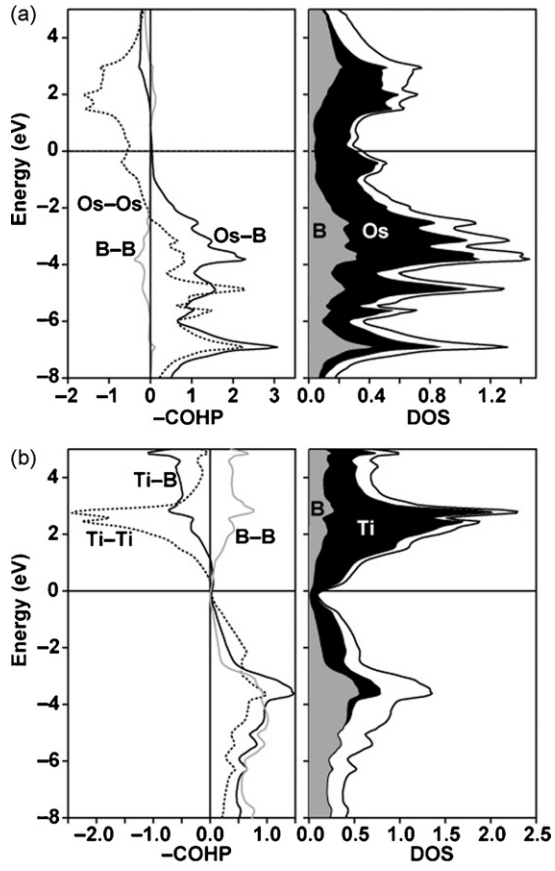

Fig. 4. (a) COHP bonding analysis of Os–B and Os–Os interactions present in OsB (left) and its partial (filled) and total DOS curve (right); (b) COHP bonding analysis of B–B, Ti–B and Ti–Ti interactions present in TiB_2 (left) and its partial (filled) and total DOS curves (right). The Fermi level has been set to the energy zero.

Os–B contact (−3.20 eV/bond) is more than twice as large as the value obtained for the Os–Os contact (−1.09 eV/bond). The ICOHP value (−3.20 eV/bond) of the Os–B interaction is also comparable with the average values (−2.82 eV/bond) and (−3.00 eV/bond) obtained, respectively, in the ternary $Ti_{1.6}Os_{2.4}B_2$ [30] (electronic structure calculations made in this work) and in the quaternary $Ti_{1.6}Os_{1.4}RuB_2$ [31]. The very low ICOHP value (−0.05 eV/bond) obtained for the average B–B distances shows the insignificance of the B–B interaction, as could be expected for the rather long B–B distance (2.87 Å). Thus, the COHP (and ICOHP) analyses confirm the electron localization function (ELF) analyses, which indicate partially covalent bonding between Os and B and no bonding between the boron atoms [11]. Nonetheless, no bonding analysis was carried out by the authors for the Os–Os distance. The COHP analyses show that these interactions are very significant and therefore contribute to weaken the Os–B interaction, which according to the ELF analysis is only *partially* covalent bonding. Because of the non-vanishing DOS at the Fermi level (see Fig. 4a, right), OsB is predicted to be a good metallic conductor.

Let us now switch to the other binary boride (TiB_2) and compare its structure with that of OsB. TiB_2 crystallizes within the AlB_2-type structure (space group *P*6/*mmm*), which is also related to OsB structure (WC-type). The difference between the OsB and TiB_2 structures probably originates from the size difference between osmium and titanium. In fact, because the titanium atomic radius (r_a = 1.448 Å) is much larger than that of osmium (r_a = 1.338 Å), the trigonal prism built up by the titanium atoms is also much larger than that of the osmium atoms. This argument is further reinforced by the fact that TiB crystallizes with both the NaCl and FeB structure types [32,33] but not within the WC-type structure like OsB. On the other hand, OsB_2 crystallizes within the orthorhombic RuB_2-type structure [29] instead of the hexagonal AlB_2-type structure like TiB_2. The valence electron (VE) count also plays an important role as was demonstrated in an earlier work [34] on the WC-type structure. In this work it was found that phases preferentially adopt the WC-type structure when their valence electron count is ten or more (OsB has 11 VE), whereas phases with nine or less valence electrons prefers the NaCl structure (TiB has 7 VE). In contrast to the OsB structure, the centers of the face-connected prisms are at a sufficient distance to allow for a B–B bonding in the TiB_2 structure, leading to the formation of a boron layer. Consequently, the structure of TiB_2 is built up of boron-filled face-sharing trigonal prisms of titanium atoms (see Fig. 3b). Thus, there should be three types of bonds in the structure: Ti–Ti, Ti–B, and B–B. From the COHP curves in Fig. 4b (left) it is obvious that Ti–Ti and Ti–B interactions are optimized in TiB_2: bonding orbitals are filled and antibonding orbitals are empty. Nonetheless, the COHP curve of the B–B interaction shows virtual bonding levels seen in the conduction band about 1 eV above the Fermi level (Fig. 4b, left). The B–B bonding is very strong, with the highest energy integral (ICOHP = −4.04 eV/bond). A trigonal planar B_4 unit, which can be the starting point for building the boron layer in TiB_2 (see Fig. 5), was found for the first time in $Ti_{1.6}Os_{1.4}RuB_2$ [31] and later confirmed in isotypic $Ti_{1.6}Os_{2.4}B_2$ [30]. COHP analyses of this B_4 unit show strong bonding with ICOHP values of −3.37 eV/bond in the ternary $Ti_{1.6}Os_{2.4}B_2$ and −3.13 eV/bond in the quaternary $Ti_{1.6}Os_{1.4}RuB_2$. This suggests that the B–B interactions in the boron layer of TiB_2 are even stronger than those present in the B_4 unit, with an energy gain of −0.67 eV/bond (approximately −65 kJ/mol, if compared with the B_4 unit present in the ternary $Ti_{1.6}Os_{2.4}B_2$). This could have been expected because in the B_4 unit the B–B bond is slightly weakened by its (small) partial ionic character, whereas in the boron layer the B–B bond is purely covalent. The occurrence of B–B bonding interactions has weakened the Ti–B bond for which an ICOHP value of only −1.80 eV/bond is observed. The fact that most of the electron density has been engaged in the formation of the Ti–B and B–B bonds leaves only weak bonding

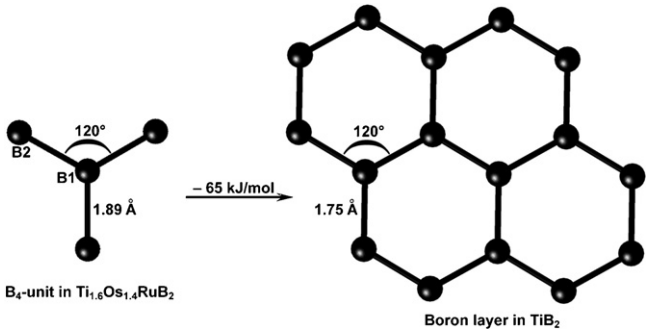

Fig. 5. The trigonal planar B_4 unit in $Ti_{1.6}Os_{2.4}B_2$ (left) is the fundamental starting motif for generating the boron layer structure in TiB_2 (right). The process leads to an energy gain of roughly −65 kJ/mol.

between the titanium atoms. Indeed an average energy integral (ICOHP) of only −0.82 eV/bond is found for the Ti–Ti interaction. The bonding in TiB_2 was also studied by Vajeeston et al. [35] and Han et al. [36] using, respectively, the TB-LMTO-ASA method and first-principles total-energy pseudopotential method, both based on density-functional theory. They found a combination of ionic, covalent and metallic bonding in TiB_2. The DOS curve of TiB_2 (see Fig. 4b) shows a pseudogap at the Fermi level, but some occupied states are still present indicating weak metallic conductivity. The electronic band structure (not shown) reveals anisotropic electrical conductivity (in the titanium layer) for TiB_2 originating from the titanium *d* electrons.

4. Conclusion

We have been able to synthesize the binary transition-metal borides OsB and TiB_2 using metallic tin as a flux agent. Phase-pure TiB_2 was obtained as a very fine polycrystalline powder, whereas OsB contains some amount of unreacted elemental osmium. COHP bonding analyses show strong B–B bonding in TiB_2 but no B–B interactions in OsB, as expected. DOS curves indicate that both phases are metallic conductors.

Acknowledgments

The authors thank Deutsche Forschungsgemeinschaft for financial support and Resi Zaunbrecher (IPC, RWTH Aachen) for the EDX analyses.

References

[1] V.V. Brazhkin, A.G. Lyapin, R.J. Hemley, Phil. Mag. 82 (2002) 231.
[2] H. Cynn, J.E. Klepeis, C.-S. Yoo, D.A. Young, Phys. Rev. Lett. 88 (2002) 135701.
[3] F. Occelli, D.L. Farber, J. Badro, C.M. Aracne, D.M. Teter, M. Hanfland, B. Canny, B. Couzinet, Phys. Rev. Lett. 93 (2004) 095502.
[4] T. Kenichi, Phys. Rev. B 70 (2004) 012101.
[5] B.R. Sahu, L. Kleinman, Phys. Rev. B 72 (2005) 113106.
[6] R.W. Cumberland, M.B. Weinberger, J.J. Gilman, S.M. Clark, S.H. Tolbert, R.B. Kaner, J. Am. Chem. Soc. 127 (2005) 7264.
[7] P. Villars, K. Cenzual, Pearson's Crystal Structure Database for Inorganic Compounds (on CD-ROM), Version 1.0, Materials Park, OH, USA, 2007/8.
[8] H. Gou, L. Hou, J. Zhang, H. Li, G. Sun, F. Gao, Appl. Phys. Lett. 88 (2006) 221904.
[9] Y. Liang, J. Zhao, B. Zhang, Solid State Commun. 146 (2008) 450.
[10] (a) D.L. Novikov, A.L. Ivanovskii, V.A. Gubanov, Zh. Neorg. Khim 33 (1988) 2673; (b) R.M. Minyaev, R. Hoffmann, Chem. Mater. 3 (1991) 547.
[11] Q. Gu, G. Krauss, W. Steurer, Adv. Mater 20 (2008) 3620.
[12] P. Schwartzkopf, R. Kieffer, Refractory Hard Metals: Borides, Carbides, Nitrides and Silicides, Macmillan, New York, 1953.
[13] L. Chen, Y. Gu, Y. Qian, L. Shi, Z. Yang, J. Ma, Mater. Res. Bull. 39 (2004) 609.
[14] M.X. Guo, M.P. Wang, K. Shen, L.F. Cao, Z. Li, Z. Zhang, J. Alloys Compd. 460 (2008) 585.
[15] L. Baca, N. Stelzer, J. Eur. Ceram. Soc. 28 (2008) 907.
[16] M.G. Kanatzidis, R. Pöttgen, W. Jeitschko, Angew. Chem. Int. Ed. 441 (2005) 6996.
[17] I. Higashi, T. Atoda, J. Cryst. Growth 7 (1970) 251.
[18] K. Nakano, H. Hayashi, J. Cryst. Growth 24/25 (1974) 679.
[19] S. Dallaire, J.-G. Legoux, Mater. Sci. Eng. A 183 (1994) 139.
[20] J. Rodriguez-Carvajal, FULLPROF, Version 2.8, ILL, July 2004, unpubished.
[21] O.K. Andersen, Phys. Rev. B 12 (1975) 3060.
[22] O.K. Andersen, in: P. Phariseau, W.M. Temmerman (Eds.), The Electronic Structure of Complex Systems, Plenum, New York, 1984.
[23] O.K. Andersen, O. Jepsen, Phys. Rev. Lett. 53 (1984) 2571.
[24] G. Krier, O. Jepsen, A.O. Burkhardt, K. Andersen, The TB-LMTO-ASA program, version 4.7, Max-Planck-Institut für Festkörperforschung, Stuttgart, Germany.
[25] S.H. Vosko, L. Wilk, M. Nusair, Can. J. Phys. 58 (1980) 1200.
[26] J.P. Perdew, J.A. Chevary, S.H. Vosko, K.A. Jackson, M.R. Pederson, C. Fiolhais, Phys. Rev. B 46 (1992) 6671.
[27] R. Dronskowski, P.E. Blöchl, J. Phys. Chem. 97 (1993) 8617.
[28] R. Dronskowski, Computational Chemistry of Solid State Materials, Wiley-VCH, Weinheim, New York, 2005.
[29] B. Aronsson, Acta Chem. Scand. 17 (1963) 2036.
[30] B.P.T. Fokwa, R. Dronskowski, Z. Anorg. Allg. Chem. 634 (2008) 1955.
[31] B.P.T. Fokwa, J. von Appen, R. Dronskowski, Chem. Commun. (2005) 4419.
[32] I.V. Brettser-Portnov, V.V. Pakholkov, S.I. Alyamovskii, Y.G. Zainulin, Russ. J. Inorg. Chem. 35 (1990) 962.
[33] B.F. Decker, J.S. Kasper, Acta Crystallogr. 7 (1954) 77.
[34] S.D. Wijeyesekera, R. Hoffmann, Organometallics 3 (1984) 949.
[35] P. Vajeeston, P. Ravindran, C. Ravi, R. Asokamani, Phys. Rev. B 63 (2001) 045115.
[36] Y.F. Han, Y.B. Dai, D. Shu, J. Wang, B.D. Sun, J. Alloys Compd. 438 (2007) 327.